JET–P(97)52

JET and the Road to ITER

P R Thomas, V P Bhatnagar and the JET Team.

JET Joint Undertaking, Abingdon, Oxfordshire, OX14 3EA,

Preprint of a paper to be submitted for publication in “Transactions of Fusion Technology” as
the proceedings of the 3rd Carolus Magnus, Summer School,
Spa, Belgium, September 1997

December 1997

ABSTRACT

JET experimental results directly relevant to ITER design are presented. From recent experiments in DT mixtures varying from 100:0 to 10:90, it is inferred that an inverse mass dependence should be included in the H-mode power threshold scaling. Using ITER similarity experiments, the global energy confinement time in JET discharges with type I ELMs is found to be consistent with the gyro-Bohm physics form which has no dependence on plasma β. This form has a weak negative mass dependence but a stronger density dependence than the ITERH93-P scaling. Using the JET MkIIa pumped divertor with N_2 seeding, ITER-relevant highly radiative regimes (P_R up to 75%) accompanied by type III ELMs have been studied. It is found that the confinement degrades progressively with increasing radiative power fraction. Power loading of divertor tiles with type I ELMs appears to be excessive with NBI whereas it is less of a concern with ICRH. Preliminary assessement of the ITER reference second harmonic ($2\omega_{CT}$) ICRH scenario with and without the addition of a small amount of He3 is also presented. High performance optimised shear discharges with potentially 'well aligned' bootstrap current scenarios consistent with ITER-relevant steady-state operation have also been studied. Internal transport barriers featuring peaked plasma profiles have been demonstrated in DT plasmas in JET. Preliminary results of a-particle driven toroidal Alfven eigenmodes (TAEs) in the 'after-glow' of NBI heated 50:50 DT plasmas are also presented.

I. INTRODUCTION

The essential objective of JET, as laid out in its design document [1], was "to obtain and study plasma in conditions and dimensions approaching those needed in a fusion reactor". This involved work in four main areas:

(i) Study of the scaling of plasma behaviour as parameters approach the reactor range;
(ii) Study of the plasma-wall interaction in these conditions;
(iii) Study of plasma heating; and
(iv) Study of α-particle production, confinement and consequent plasma heating.

This objective and the areas of work defined the main parameters of the JET device and the facilities that would be required. In particular, α-particle production and confinement not only necessitates the tritium plant and remote handling facilities but also sets a minimum plasma current of around 3MA. In view of its scale and DT compatibility, JET is the closest approach to ITER, or any other next step, and so is central to the world fusion programme.

A shift in emphasis was formalised [2] for the extension of the JET programme 1996-99 thus: "The purpose of the extension is to provide data of direct relevance to ITER, especially for the ITER-EDA, before entering a final phase of D-T operation. In particular, the extension would:

(i) Make essential contributions to the development and demonstration of a viable divertor concept for ITER; and

(ii) Carry out experiments using deuterium-tritium plasmas in an ITER-like configuration, which will provide a firm basis for the D-T operation of ITER; while allowing key ITER-relevant technology activities, such as the demonstration of remote handling and tritium handling, to be carried out".

Before embarking on a description of JET's results, it is useful to discuss the ITER objectives [3]. This puts the JET results in their proper context and a selection of topics for presentation.

The ITER objectives are:

(i) To demonstrate controlled ignition and extended burn of DT plasmas;

(ii) To pursue steady state operation as a long-term goal;

Table 1: JET and ITER Parameters

Parameter	Units	JET		ITER/EDA
		Original 1983-91	**Divertor 1994 onwards**	
Typical major radius	m	2.96	2.85	8.1
Typical minor radius	m	1.2	0.95	3
Plasma elongation		1.6	1.8	1.6
Toroidal magnetic field on axis	T	3.45	3.6 3.8 (1997)	5.7
Plasma current	MA	≤7	≤6	21
Flat top pulse length	s	20-60	0-60	1000
Transformer flux	Wb	34	42	608
NBI power	MW	20	22	Heating methods to be chosen
ICRH power	MW	15	17	
LHCD power	MW	3 (1991)	10	
ECRH power		–	–	
Divertor Configuration		SN(D), SN(U), (DN)	SN(D), SN(U), (DN)	SN(D)

SN= single null X-point, D=down, U=up, DN=double null

(iii) To demonstrate technologies essential to a reactor in an integrated system; and

(iv) To perform integrated testing of high heat flux and nuclear components required for a fusion reactor.

The most significant contributions which JET can make to ITER are associated with the first two objectives. JET is able to make ITER-like plasmas on a scale closest to ITER and is unique for its DT capability. Thus, JET results are pivotal in projections of ITER performance

and its operating margin.

The contribution which JET can make to the last two is obviously more limited. JET has gained considerable experience in both tritium handling [4] and remote handling [5]. Differences in the extent and continuity of operation mean that the main impacts are those of “in principle” demonstrations; for example, the separation of tritium from the exhaust stream of JET plasmas, using a closed system, shows that it is possible in practice and allows a system for ITER to be designed with confidence. Also, JET has a high heat flux test facility [6] and is the only tokamak using beryllium [7] in plasma facing components. Thus it is able to make effective contributions to the design of ITER’s high heat flux components.

The main parameters of the JET tokamak are given given in Table 1 where the ITER-EDA [3] design parameters are also included for comparison. The auxiliary heating power in JET includes the neutral beam injection (NBI) power of 21 MW (from 2 beam boxes out of which one has been used to inject tritium), 17 MW of ion cyclotron resonance heating (ICRH) power and 7 MW of Lower Hybrid Current Drive (LHCD) power. JET has a single null (bottom X-point) divertor configuration. A wide-angle view of the in-vessel components of JET at the restart of operation of JET in 1997 is given in Fig. 1 where some of the items such as divertor target plates, ICRH antennas, LHCD launcher etc. can be identified. To determine the core and divertor plasma parameters, there is a large number of diagnostics [8] in and around the machine. These are notable for their tritium compatibilty and their ability to operate with an intense 14 MeV neutron flux. JET plans to carry out DT experiments in two stages: DTE1 (1997) and

FIG. 1. A view of the in-vessel components of JET (1997) with MkIIa divertor on the floor of the torus. On the right hand side, an array of 4 ICRH antennas adjacent to the LHCD launcher and a poloidal limiter can be seen.

DTE2 (1999). In view of limited neutron budget during DT operations, automatic feedback real-time control systems have been implemented so that if the desired performance is not achieved at expected time during the discharge, the plasma shot is terminated with a soft landing thus saving neutrons. Also, certain given plasma parameters can be maintained at a programmed level by a system controlling, in real time, a number of auxiliaries such as NB, ICRH, LHCD etc. Using digital techniques, ICRH or NBI power delivered to the plasma can be controlled with precision. The JET control and data acquisition system is based on a network of dedicated minicomputers (in UNIX environment) which provide centralised control, monitoring and data acquisition on CAMAC and VME standards.

The ITER-relevant JET experiemental results are presented in Section 2. These include scaling of H-mode threshold power, energy confinement scaling in dimensionless parameters in H-modes with type I ELMs, divertor operation in highly radiating regimes with type III ELMs, ICRF heating regimes, high performance optimised shear scenarios and a preliminary observation α-particle driven TAE modes. Discussion and conclusions of this paper are contained in Section 3.

II. EXPERIMENTAL RESULTS

JET energy confinement results have played a leading role in fixing the main ITER parameters. In order to achieve its first objective, ITER must be able to access the H-mode, have an adequate confinement margin for ignition, and be stable during the plasma burn. Each of these areas will now be described in turn.

A. H-Mode Threshold Power

The H-mode threshold power has been observed in all machines to be proportional to toroidal field strength, and, above a minimum value, nearly proportional to electron density [8-10]. This is summarised in figure 2 [10], where the threshold power has been compared to a dimensionally correct scaling form. The contributions from each machine are labelled and it may be seen that JET data points stand out on the upper right hand side. The data permit a range in the exponent of density from 0.5 to 1.0 and this leads to most of the uncertainty in the projection to ITER. For example, at a density of 5×10^{19} m^{-3}, the projected value for the H-mode threshold ranges from 50 to 200 MW, to be compared with an auxiliary heating power of 100 MW provided in the ITER design. The uncertainty is exacerbated by the data variability, even within a single machine's data set. The source of this variability appears to be due to a number of factors, including details of configuration and conditioning, and is under investigation.

JET has prepared a range of "ITER similarity pulses" for confinement studies at toroidal field and plasma current varying between 1 T/1 MA to 3.8 T/3.8 MA. These are operated with a 2-3 s long heating power ramp or staircase so that the H-mode threshold can be measured at the

same time. These carefully controlled and identically configured pulses result in a tighter comparison with the scaling law, as shown in figure 3. This underlines the importance of careful control of experimental conditions for obtaining consistent results. Improvements to the JET threshold dataset will be obtained in association with further confinement scaling experiments. In particular, it is hoped that the density dependence can be pinned down more precisely.

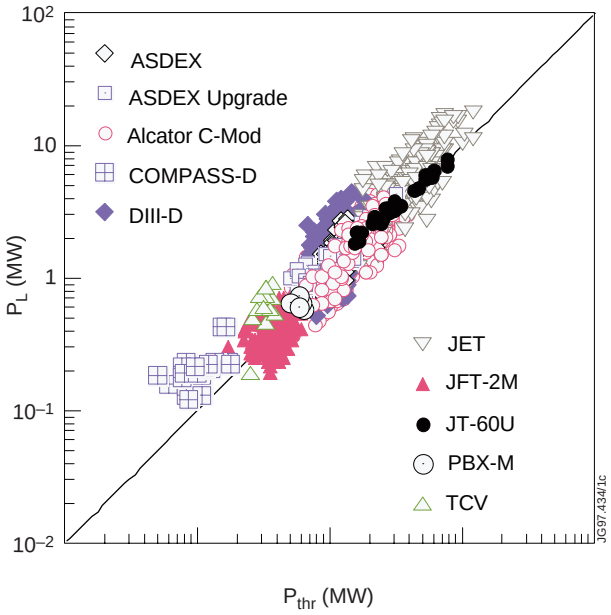

FIG. 2. A multi-machine power threshold database in which loss power is plotted against the L-H mode threshold power Montreal scaling [10] $P_{thr} = 0.45\ B_T\ n_e^{0.75}\ R^2$ (MW, T, 10^{20} m^{-3}).

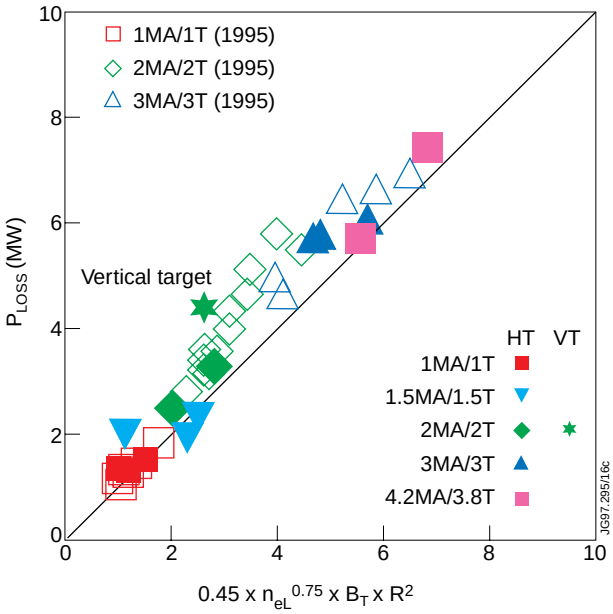

FIG. 3. The JET threshold power database obtained in controlled ITER similarity discharges. Here, loss power is plotted with the same scaling as in Fig. 2.

JET is in a unique position to determine the sensitivity of the H-mode threshold to the tritium content of the plasma. JET has completed its first phase of the DTE1 experiments. From these experiments, as an illustration, in figure 4, we show time traces of three shots in three different D/T gas mixtures 100:0, 50:50 and 10:90. ICRH power is ramped up slowly (3 s) and D_α-signal is monitored for the appearance of threshold ELMs. These plasmas at 2.6T/2.6MA were heated with H-minority ICRH at 42 MHz. As indicated on the figure, H-mode threshold occurs at lower power levels when tritium concentration in the plasma increases from 0 to 90%.

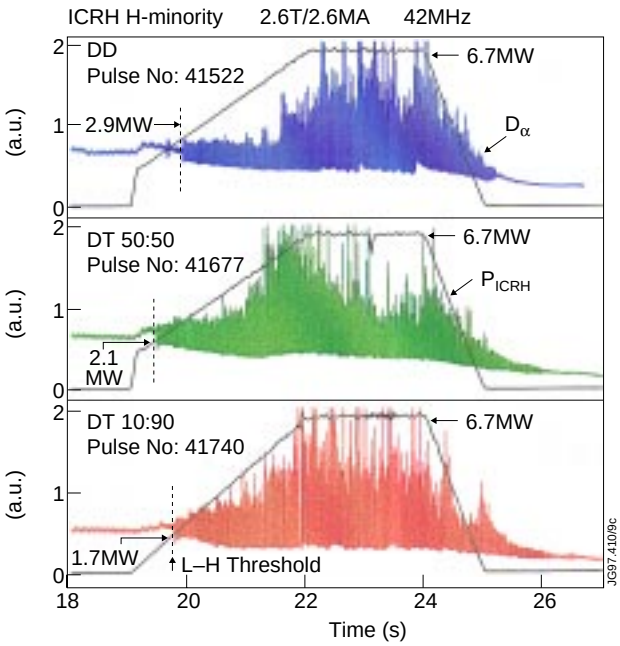

FIG. 4. Observation of mass dependence of H-mode thresholds with D_α-signal in three similar shots with three different mixtures of D/T concentrations as indicated. These plasmas were heated by ICRH with a slow power ramp up as shown.

In figure 5, we plot loss power as a function of an earlier Montreal [10] H-mode scaling for a range of plasma current and magnetic field in ITER relevant discharges in DD and two other DT mixtures as indicated on the figure. The 45°-line is drawn for the above Montreal scaling which does not include a mass dependencce. Note that the DT data points lie below the line while the deuterium points are close to it. In order to include the isotopic mass dependence in the scaling, a regression analysis has been done using the same power exponents as in [10] but with an isotopic mass parameter A_{eff} which is weighted by the relative DT concentration [11]. The threshold power data shows roughly an inverse mass dependence (see the horizontal axis in figure 6).

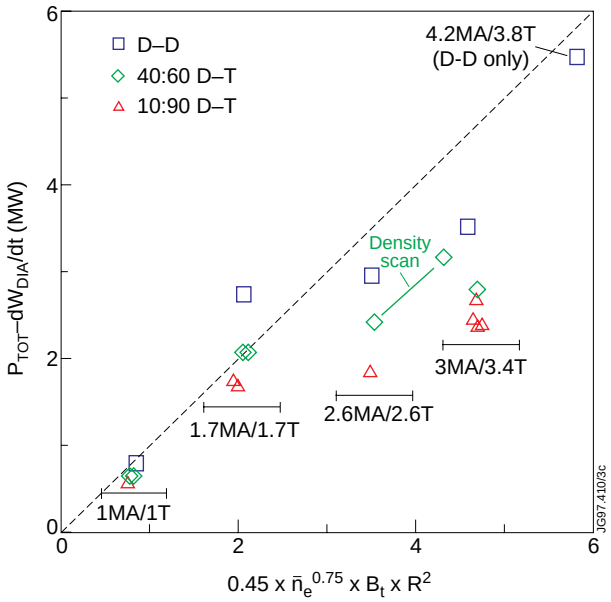

FIG. 5. Plasma loss power at the L-H transition as a function of the Montreal ITER scaling [10] for three different D/T mixtures in JET plasmas as indicated. The D/T data points are below the line suggesting the need of a new scaling with a mass parameter in it.

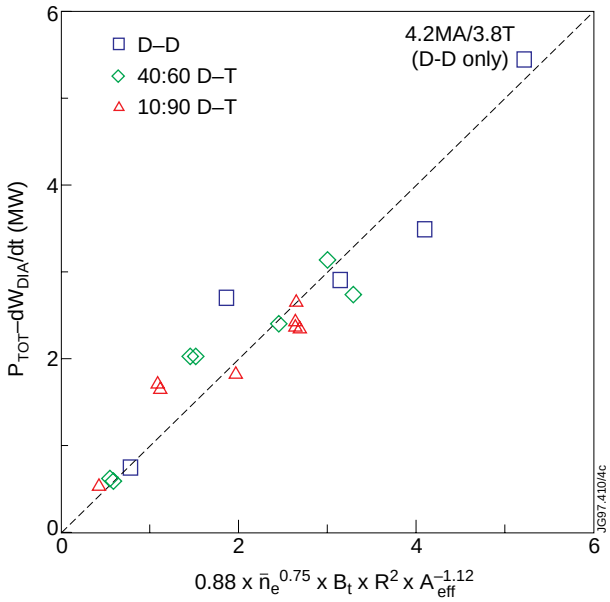

FIG. 6. A new fit to the JET H-mode threshold power data (see Fig. 5) with the same power coefficients as in Ref. 10 but with a mass dependence. Approximately, an inverse mass scaling is inferred.

The above results of lower power threshold in DT plasmas are independent of heating method. Not only is this welcome news for ITER but it also should help to reveal the underlying physics. Future JET experiments on the H-mode threshold will be concentrated upon a better determination of the density dependence, an improvement in the isotopic scaling by conducting experiments in H- plasmas after DT operation and an improvement of edge diagnosis. The latter is important both to pin down the H-mode mechanism and to remove the part of threshold variability due to conditioning and profile effects.

B. Energy Confinement Time

Since it is proposed to operate ITER in the ELMy (type I) H-mode, most of JET's recent activities in studying energy confinement have been in this regime. Previously, data has been provided for L-mode [12] and ELM-free H-mode [13] databases. A regression scaling law for energy confinement has been obtained with the ITER ELMy H-mode data base [14], which is shown in figure 7. Once again, the importance of JET data is apparent from this figure. The resulting scaling law,

$$\tau_{th}^{ELMy} = 0.029\, I_p^{0.90}\, B_T^{0.20}\, P_L^{-0.66}\, A^{0.20}\, R^{2.05}\, N_e^{0.40}\, \varepsilon^{0.19}\, \kappa^{0.92} \qquad (1)$$

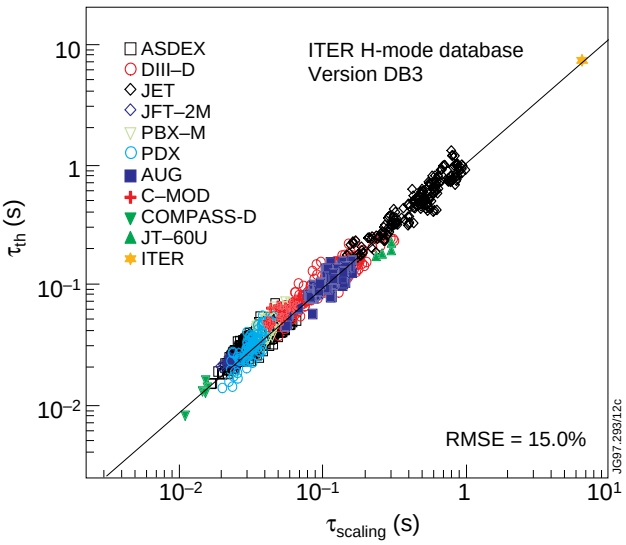

FIG. 7. A multi-machine database of experimental thermal energy confinement plotted as a fucntion of ELMy H-mode scaling [14] given in Eq. 1.

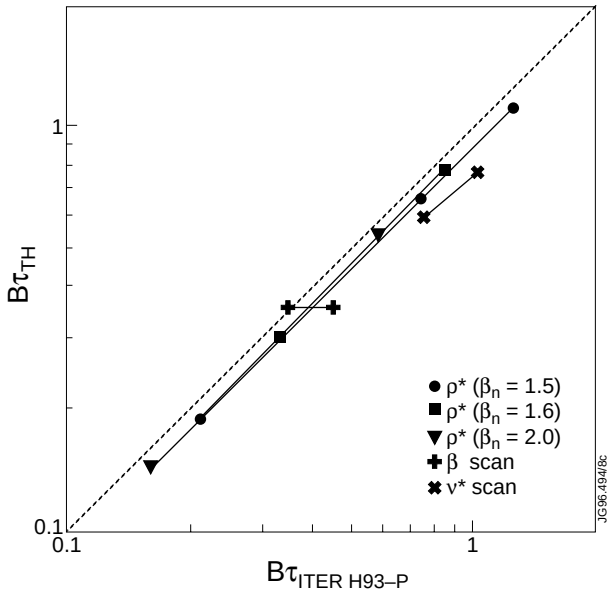

FIG. 8. Normalized thermal confinement time is plotted as a function of B $t_{ITERH93\text{-}P}$ scaling for ρ, ν* and β-scans. B represents the cyclotron frequency.*

is written entirely in "engineering parameters". Here, I_p is the plasma current, B_T is the toroidal field, P_L is the loss power, M is the relative ion mass, R is the tokamak major radius, N_e is the electron density, ε is the inverse aspect ratio and κ is the plasma elongation. This does not allow a particularly transparent connection with physical models, although it does happen to comply with Connor-Taylor constraints [15]. For this reason, subsequent work has concentrated upon "similarity experiments", particularly in conjunction with DIII-D, in order to pick out the dependence of energy confinement on physical parameters such as ρ* (= ρ_i/a), ν* (= $\nu_e a/v_{the}$) or β (= $2m_0\langle p\rangle/B_T^2$) where ρ_i is the ion Larmor radius, a is the plasma radius, ν_e is the electron-ion collision frequency, v_{the} is the ion thermal velocity, and <p> is the average plasma pressure. The energy confinement times of some of these similarity pulses [16] are shown in figure 8 and are compared with the ELM-free version of the ITERH93-P scaling which can be written as

$$B\tau_E \sim \rho^{*-2.7}\, \nu^{*\,-0.28}\, \beta^{\,-1.2} \qquad (2)$$

where B represents cyclotron frequency. The fitting of JET data with this scaling shown in Fig. 8 gives a clear indication of where the main sensitivity of extrapolation to ITER lies! The ρ^* dependence of the scaling law is in good agreement with that obtained in the similarity experiments. Also, although over a very limited range in τ_E, the ν^* dependence seems to be confirmed. However, the similarity experiments display almost no sensitivity on β, which contrasts sharply with the strong dependence in the ITERH93-P scaling law. From recent studies, it seems likely that the β dependence in the scaling law is an artefact of the dataset. In particular, there is a strong correlation between β and machine aspect ratio which, when factored in, permits a range of exponents for β, including zero. Thus, it is likely that the weak dependence on β, revealed by the similarity experiments, is correct.

More recent experiments of D-beam into T-plasmas have been compared with D-beams in D-plasmas. The JET DT data does not fit the mass scaling in either the ELMy ITERH93-P ($\propto A^{0.3}$) or the ELM-free ITERH93-P ($\propto A^{0.41}$) scaling. In fact, the above D$\rightarrow$D and D$\rightarrow$T data fits better with the physics form of the gyro-Bohm scaling [17].

$$B\tau_E \sim \rho^{*-3}\, \nu^{*\,-0.3}\, \beta^{0} \qquad (3)$$

The mass and density dependence in the gyro-Bohm physics form and the ITERH93-P scaling can be explicitly written [18] as

$$\tau_E \text{ (gyro-Bohm)} \propto n^{\,0.32}\, A^{-0.25} \qquad (4)$$

and

$$\tau_E \text{ (ITERH93-P)} \propto n^{\,0.17}\, A^{-0.41} \qquad (5)$$

A fit to the above JET ELM-free data [18] is shown in figure 9. This preliminary analysis suggests that for ITER, the adverse mass dependence in the gyro Bohm scaling is compensated by the better density dependence as compared to ITERH93-P.

The ITER database on β-limits shows a significant dependence on ν^*. Whereas, at high ν^* the limit is around that anticipated from ideal MHD theory, at low collisionality the maximum β is determined by low m - n islands, which have been identified as neo-classical tearing modes [19]. In contrast, JET data [20] do not exhibit this behaviour, as shown in figure 10. This has been variously interpreted as being due to the high β phase being too short or the sawteeth not being strong enough to seed the islands.

A number of further confinement issues have emerged which are to be studied in an experimental period after DTE1. These include further similarity experiments, constrained to be far away from operating boundaries. Proximity to both the L-H threshold and the density limit have been observed to affect the scaling of energy confinement. The approach to these bounda-

ries will then be studied separately. It is proposed that ITER should operate with a significant proportion of power being radiated from the divertor and edge plasmas. This regime can degrade energy confinement if the radiated power fraction is too large. Thus, it is essential to study the confinement scaling, in this regime, and its dependence on the radiated power fraction. Finally, it is hoped to clarify the difference between JET and other machines in respect of stability against neo-classical tearing modes. In particular, the effect of operating with larger amplitude sawteeth will be investigated.

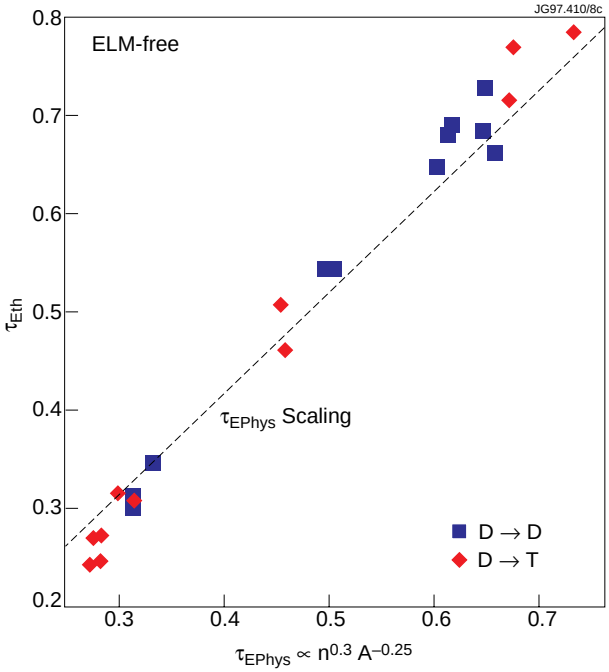

FIG. 9. Normalised thermal confinement time is plotted as a function of gyro Bohm physics scaling with a weak mass dependence ($A^{-0.25}$). A reasonably good fit with both JET DD and D/T data is obtained.

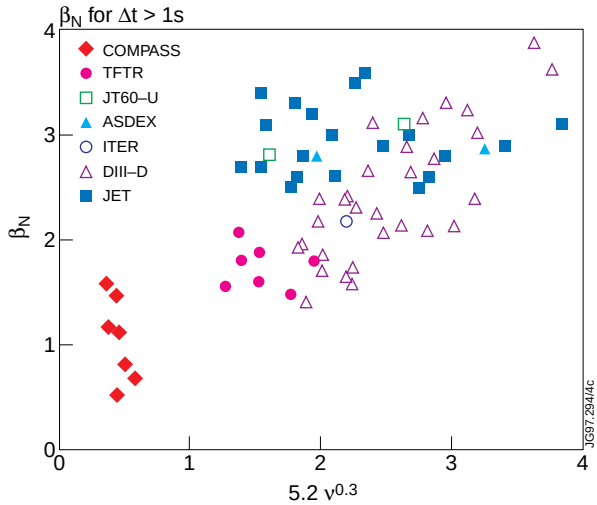

FIG. 10. A multi-machine database of achieved normalised β_N plotted against 5.2 $\nu^{0.3}$ where ν is the collision frequency.

C. Divertor Solutions for ITER

Handling the 300MW heat output from the burning plasma, whilst exhausting the helium ash and keeping plasma impurities at a low level, remains one of the most vexing parts of the ITER design. Not only must the divertor serve in this function but it must continue to do so reliably for many years. The basic scheme for doing this has been envisaged as requiring an ELMy (type III) H-mode together with a significant part of the power being radiated or charge-exchanged away, in order to spread the heat load. Variants of this scheme have been tested at JET and their properties studied.

At the heart of the JET divertor programme [21] lies a series of three target structures which are progressively more closed (figure 11). The MkI configuration was the most open and tested the operation of the divertor coils and sub-divertor cryopump. It also had the flexibility to allow a wide range of main plasma and divertor equilibria. With this facility, the relationship

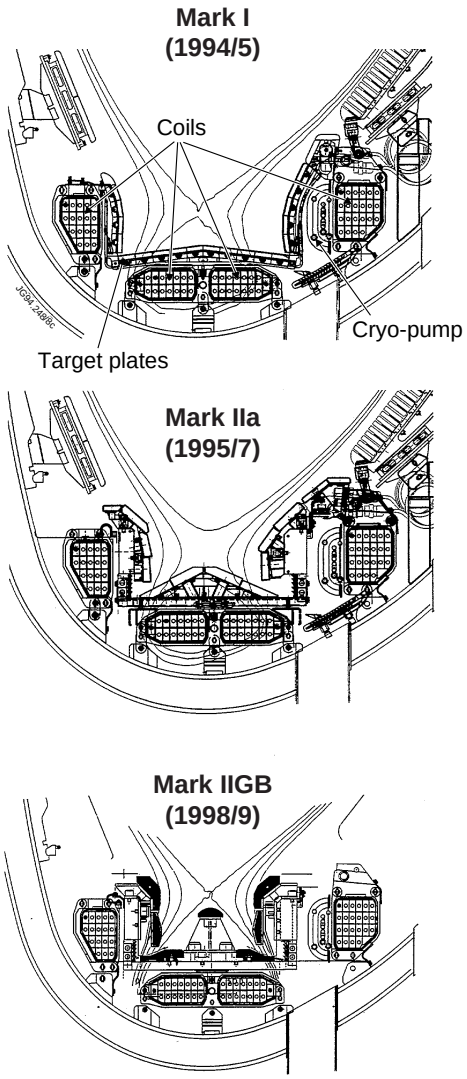

FIG. 11. A series of 3 divertor configurations installed or planned in the JET vessel. The MarkIIGB ('gas-box) will be installed after the post DTE1 experiments by remote handling.

between plasma geometry and ELM-free period was identified. In addition, the initial experiments with a radiating divertor were performed. The MkIIa divertor is currently in use. It features more closed side walls than the MkI, in order to trap neutral hydrogen, and a better conductance to the cryo-pump. The MkIIa power handling capacity is better than that of the MkI. Finally, the MkIIGB, the so-called 'gas-box', will be installed by remote handling after DTE1. Not only does it have the tightest baffling against neutrals but it has the longest divertor legs. These properties should maximise the divertor plasma atomic losses, whilst decoupling the divertor and the main plasma; so making this the most ITER relevant divertor of the three.

In the absence of a momentum sink, the pressure along the divertor field lines is constant. Thus, processes, such as atomic radiation or ionisation, which cool the plasma will increase its density. This, in its turn, enhances the cooling processes and the opacity of the divertor plasma to neutrals. In this way, it should be possible to remove most of the energy from the plasma before it arrives at the divertor target and spread it over a large surface area. This has been achieved experimentally; albeit at a cost in both main plasma confinement quality and purity. At very low target plasma temperature (≤5eV) recombination and charge exchange act as plasma momentum sinks so that the plasma flow to the target is reduced. Thus, even the ionisation power is removed from the target and the plasma 'detatches'. This regime has also been investigated with feedback control of the gas feed using the target Langmuir probes to sense detatchment.

Figure 12 shows the time history of a plasma [22] with 30MW heating power, in which more than 70% of the power is radiated by nitrogen seeding. The confinement quality H_{89} [12] indicates that this plasma is midway between a high quality H-mode ($H_{89} \geq 2$) and L-mode ($H_{89} = 1$). The confinement quality is substantially determined by the proportion of radiated power, as seen in figure 13. A number of different plasma configurations are indicated by the

different symbols. That this occurs is due in part to the radiating region shifting to the separatrix X-point and so invading the main plasma, as shown in figure 14. In addition, there is a change in the properties of the confinement barrier which results from this, which limits the plasma density and which will be described shortly. The pollution of the plasma by impurities is proportional to the radiated power as can be seen in figure 15. That there is a more or less universal scaling for Z_{eff} against radiated power and density is rather surprising since it takes no account of whether the radiation is from the main or divertor plasma.

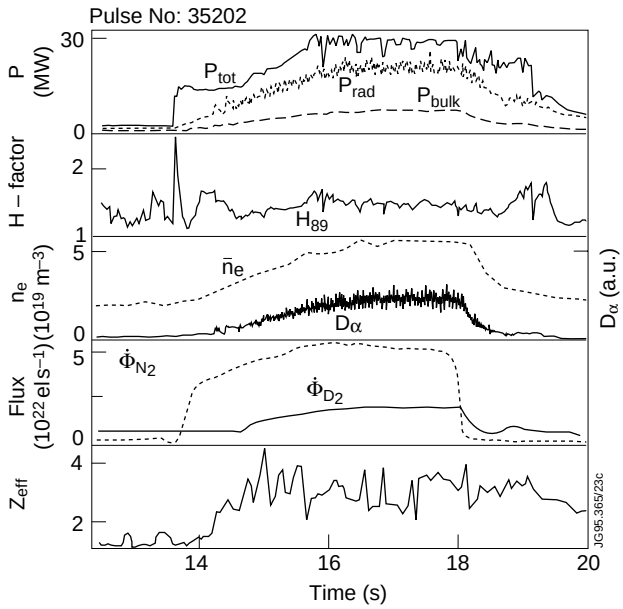

FIG. 12. A highly radiative ELMy H-mode divertor discharge produced with nitrogen injection to enhance radiation. P_{rad} and P_{tot} are the radiated and the total input power respectively. D_α refers to the Balmer α-line emission from the D-plasma and Φ_{N2} is the flux of nitrogen gas injection.

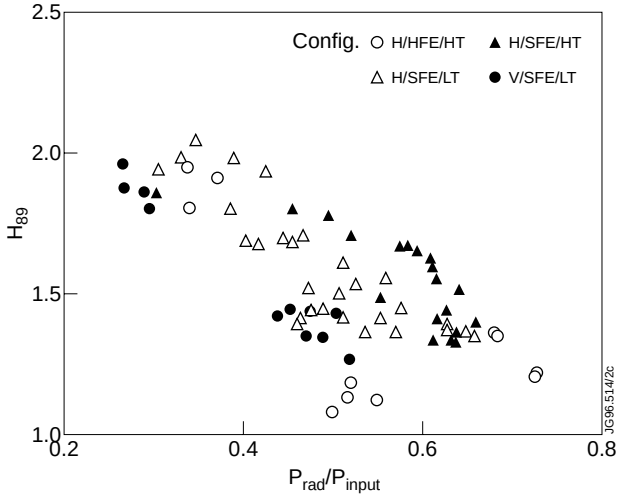

FIG. 13. Confinement quality factor H89 over L-mode [12] plotted as a function of radiated power fraction in MkIIa for four configurations with D_2 (f_{rad} < 0.45) and D_2 +N_2 puffing for higher radiated fraction. Here, H and V represent horizontal and vertical targets, HFE and SFE refer to high flux expansion and standard fat configuration and HT and LT indicate high and low triangularity respectively.

At present, the most promising regime for combining good confinement quality with steady state is the ELMy H-mode. It is of some concern to know which of type I or type III ELMs [23] is suitable for ITER in the ignition regime. Type I ELMs, produced by neutral beam heating, typically eject 5-10% of the total plasma energy content [24], as shown in figure 16, and the power loads on divertor surfaces are on the scale of GW.m^{-2}. Thus the integrity of plasma facing surfaces would be threatened. On the other hand, the type I ELMs with ICRH are much more benign [25], being of higher frequency and smaller amplitude. Type III ELMs are invariably associated with a reduction in both energy and particle confinement times. This is understood by reference to a plot of discharge trajectories in edge temperature and density [26], shown in figure 17. The type I ELMs appear as the plasma contacts the ballooning instability boundary.

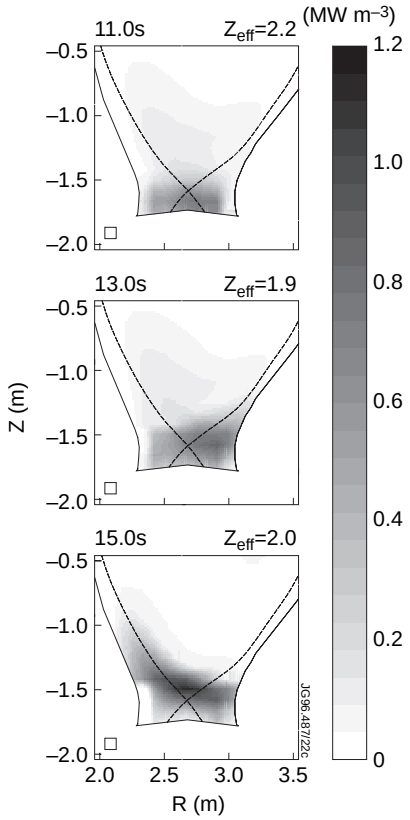

FIG. 14. Tomographic reconstruction of the total radiated power (75-80%) during detachment (pulse number 34355) at three time slices. In the bottom figure, the radiation region shifts to the X-point invading the main plasma and ultimately leading to a radiation collapse.

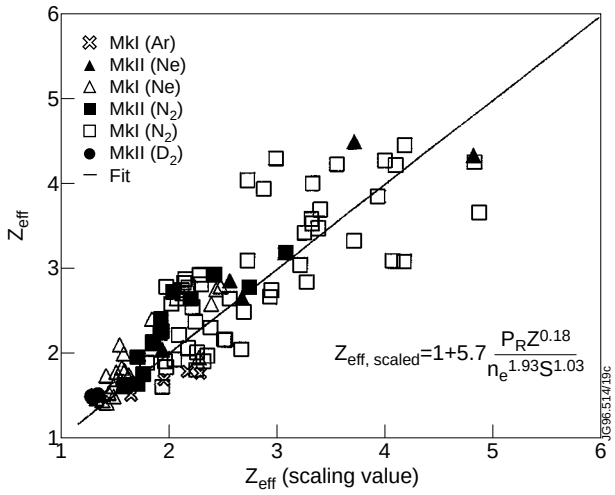

FIG. 15. Measured Z_{eff} plotted as a function of the Z_{eff} scaling (shown) for radiative discharges in Mk I and MkIIa for a variety of seed gases. Here, P_R is the radiated power fraction, Z is the charge of the impurity, and S is the surface area.

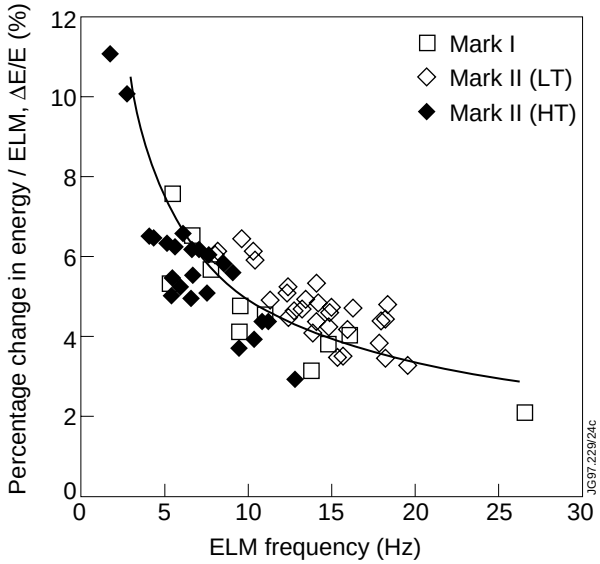

FIG. 16. Percentage drop in diamagnetic stored energy as a function of type I ELM frequency in NBI heated H-mode discharges in MkI and MkIIa divertors. LT and HT refer to low and high triangularity plasmas respectively.

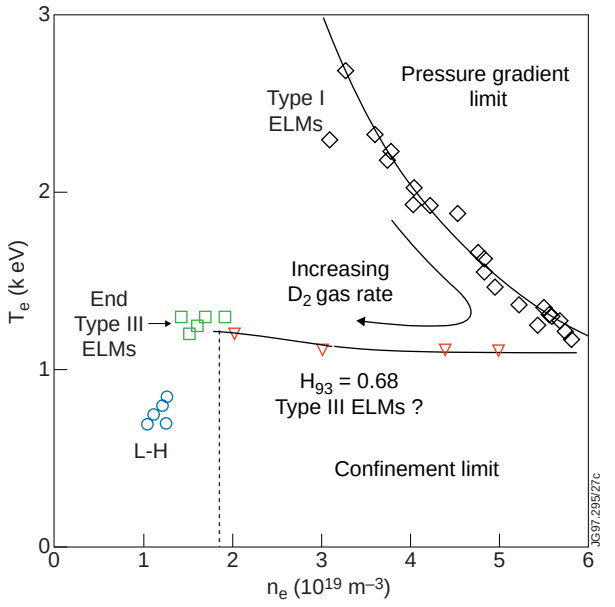

FIG. 17. Operational window in edge electron temperature and edge electron density defined by type I ELMs pressure gradient limit line and confinement degradation with type III ELMs. The path followed by edge parameters with increasing D_2 gas fuelling is also shown.

As the density is increased, the edge temperature drops until a point where the confinement is strongly degraded. This is consistent with the picture that there is a minimum temperature for the sustainment of the H-mode. The H-mode density limit is associated with this behaviour and reveals itself as a degradation in particle confinement, which can become so severe that the effective gas fuelling rate is negative.

These features of JET divertor operation will be tested in DT during the DTE1 experiment. Of particular interest will be the effect of isotopic content on the ELM behaviour, described in the last paragraph. Through its main design features the MkIIGB divertor should alleviate the problems associated with the maintenance of good confinement and a large fraction of radiated power. Indeed, if the tight baffling and long divertor legs do not result in a strong decoupling between main and divertor plasmas, the entire question of how to exhaust particles and heat from ITER will have to be revisited.

D. ICRF Heating

The JET ICRH system couples power via four antennas each made of four current straps which can be phased independently. Experiments have been performed in DT plasmas with up to 95% tritium in ITER-relevant ICRH scenarios such as T second harmonic heating ($2\omega_{CT}$), D-minority heating in T (ω_{CD}) and 1% He3 minority in T [18]. In figure 18, we show a comparison of $2\omega_{CT}$ heating with and without 1% He3 where the input power traces are very similar in the two cases. The ITERH93-P thermal confinement factor H93TH (fast-ion energy subtracted) is found to be signicantly higher with He3 added. Also, with He3, some discrete ELMs with higher amplitude, in addition to the higher frequency ELMs typical of ICRH, are found. The neutron rate, line-averaged plasma density and electron temperature are also shown. From other analysis, it is found that in discharges with 1% He3, neutrons are of thermal origin. Performance with He3 is better as in this case power deposition profile is more peaked than pure $2\omega_{CT}$ case. Also, in the latter case where the density was relatively low, a fraction of fast ions are lost due to large banana orbits.

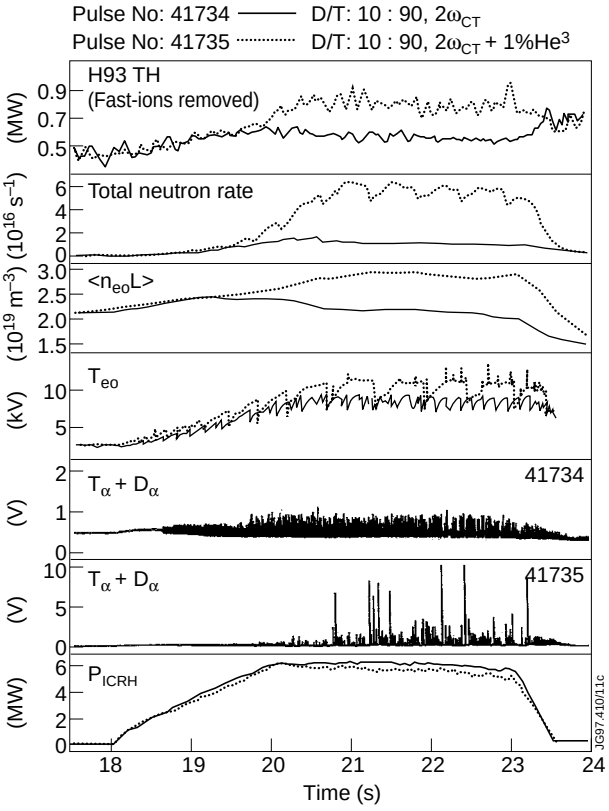

FIG. 18. A comparison of two similar ICRH discharges: one with and the other without He^3 added (1%) in $2\omega_{CT}$ heating scheme. Enhanced performance with He^3 is obtained due to more peaked power deposition profile resulting from stronger wave damping and smaller orbits.

E. Optimised Shear and Steady-State Operation

In order to keep the recirculating power to an economically low level, the bootstrap current in a steady-state tokamak reactor must be 70-80% of the total plasma current. In addition, the bootstrap current density must be 'well aligned' to that required to support the poloidal magnetic field so that a component of current drive with zero net total is not required. The reversed shear regime, where there is a minimum in the safety factor away from the magnetic axis, is able to accomplish this. The core region, with reversed magnetic shear, can be in the second stable region so that the β limit is very large (stable equlibria with β values of twice the Troyon limit have been found). This provides the bootstrap current drive. Since the maximum in current density is off axis, it can be persuaded to match the maximum pressure gradient; so providing the good alignment.

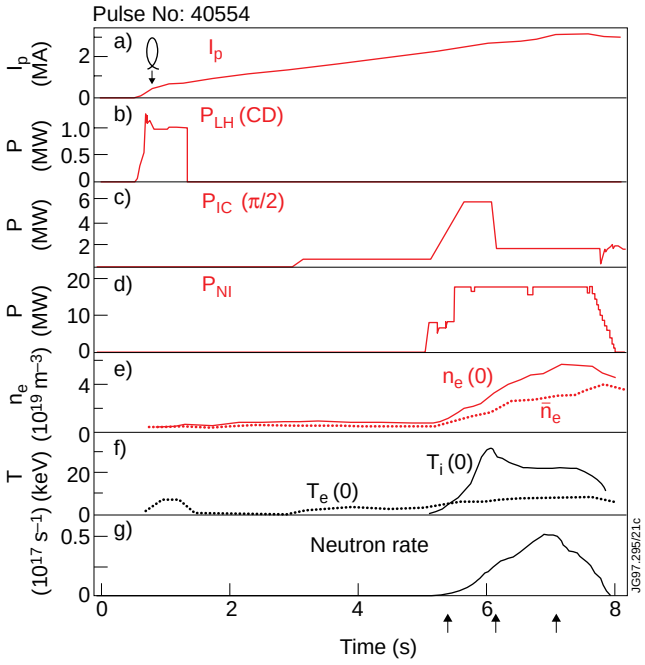

FIG. 19. Time traces of a combined NB and ICRH heating optimised shear discharge giving enhanced core confinement. Preheating with LHCD and ICRH power to control the current diffusion is also shown. Here, π/2 refers to the phasing of the ICRH antenna.

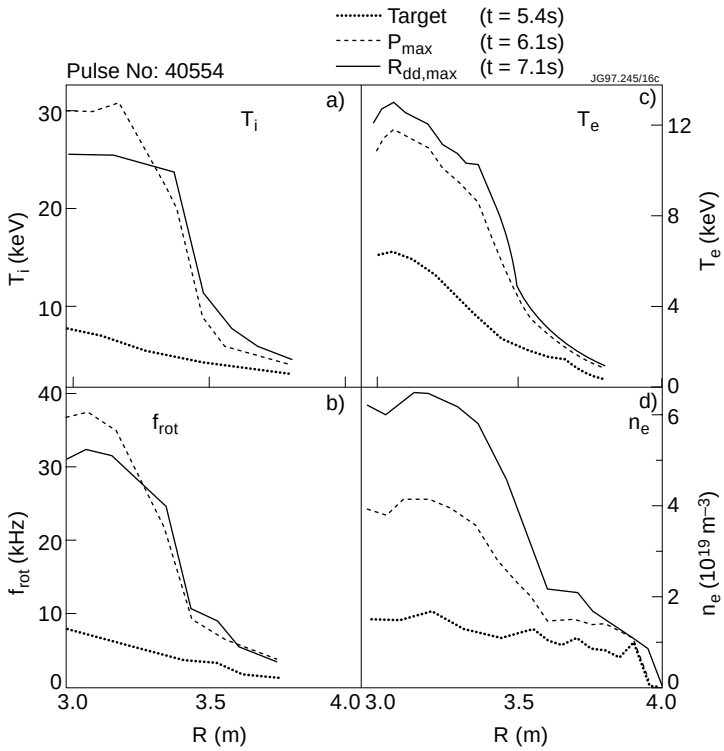

FIG. 20. Typical plasma profiles in optimised shear DD discharges in JET. (a) ion temperature, (b) electron temperature, (c) plasma rotation frequency and (d) electron density. Three profiles in each case refer to before an internal transport barrier forms (...), at peak pressure (—) and at maximum neutron rate (_).

JET, in common with a number of other machines, has made reversed shear plasmas [27]. It is found that the core region has an internal transport barrier close to the point of shear reversal and that a very good fusion performance can result. Since it is not apparent that reversed shear is actually necessary for high transient fusion performance, a flattened profile, in fact, gives the best results, the regime has been dubbed Optimised Shear at JET. Such a plasma is illustrated in figures 19 and 20. In JET, optimised shear experiments are carried out immediately after the

current rise phase of the discharge where advantage is taken of the natural delay in the current diffusion to the plasma centre as the current is ramped. The current diffusion can be further delayed by electron heating by ICRH. The target plasma has q>1 everywhere. Neutral beams and ICRH are injected at optimised times in the low target density plasmas. In such discharges, an internal transport barrier is established early in the discharge which expands outwards to approximately 2/3 of the plasma radius. These discharges have very peaked plasma temperature and density profile where the central plasma pressure has reached up to 3 bar [22] and the ion temperature are up to 34 keV. The example given in figures 19 and 20 produced the largest DD fusion output ever obtained in JET.

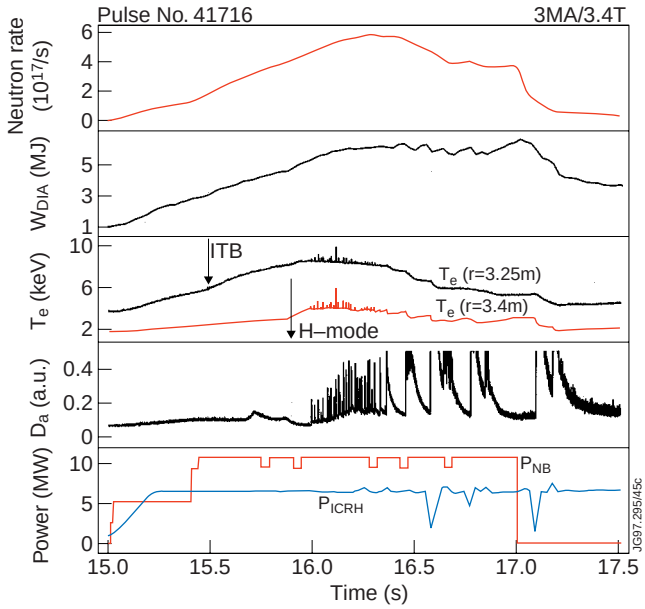

FIG. 21. Illustraion of an optimised shear discharge in DT where D-NBI and ICRH power were used in a tritium plasma. T-NBI was not used at this time. Fusion power output of 1.7 MW was obatined in this case.

Results of first attempts in which D-NBI and ICRH were used in tritium plasmas (plasma composition was DT 40:60) are shown in figure 21 where the maximum DT neutron yield was about $6x10^{17}$ n/s leading to a fusion power output of about 1.7 MW. Maximum fusion power in this regime has been about 2MW. Experiments both with D- and T-beams are imminent where much higher fusion power output (~10MW) is expected.

The internal transport barrier is so profound that the thermal conductivity [22] in the plasma core falls to levels comparable to the neoclassical values, as shown in figure 22. The plasma heat input needs to be controlled to keep the plasma away from the β–limit. Figure 23 shows the trajectory of an optimised shear plasma in the β_N versus $\beta(0)/<\beta>$ plane. As the transport barrier moves outwards, the β-limit increases because the pressure profile is less peaked. If the stability boundary is crossed, a loss of confinement or even a disruption can ensue. This indicates that profile control is going to be a major issue if these plasmas are going to be made steady state and exploited in ITER.

Following DTE1, where peak fusion performance will drive the development of optimised shear plasmas, the emphasis will change towards the preparation of steady state plasmas for ITER. If the 'well aligned' configurations show the same improvement in confinement as those made so far, there is a prospect that as well as being a steady state development, these plasmas could improve ITER's ignition margin. As remarked earlier, profile control, particularly of the safety factor, will be the key to the exploitation of the optimised shear regime. To this end, a motional Stark effect diagnostic is being installed early in 1998 which will provide a measure-

ment of the profile of poloidal magnetic field strength. An impediment to the sustainment of optimised shear plasmas is inadvertant entry into the H-mode. It is hoped that this can be controlled by use of radiating impurities such as krypton. Finally, α-ash removal will have to be demonstrated for the steady-state plasmas.

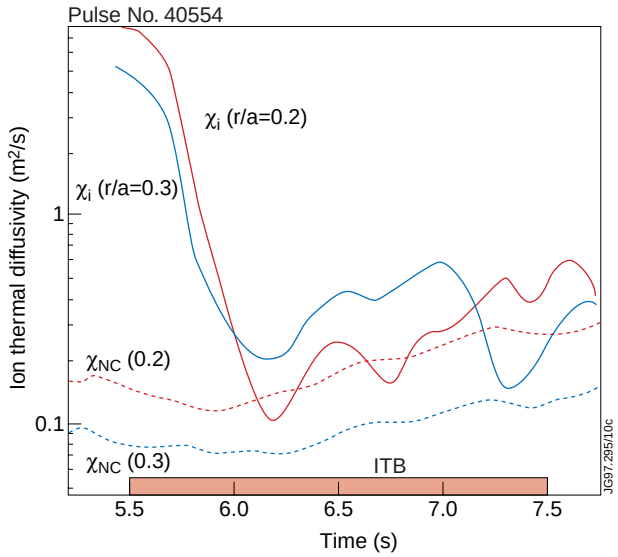

FIG. 22. Ion thermal diffusivity at two radii obtained from a TRANSP-code analysis is plotted as a function of time in the optimised shear discharge shown in figures 19 and 20. For comparison neoclassical (NC) values are also shown. ITB refers to the achievement of internal transport barrier.

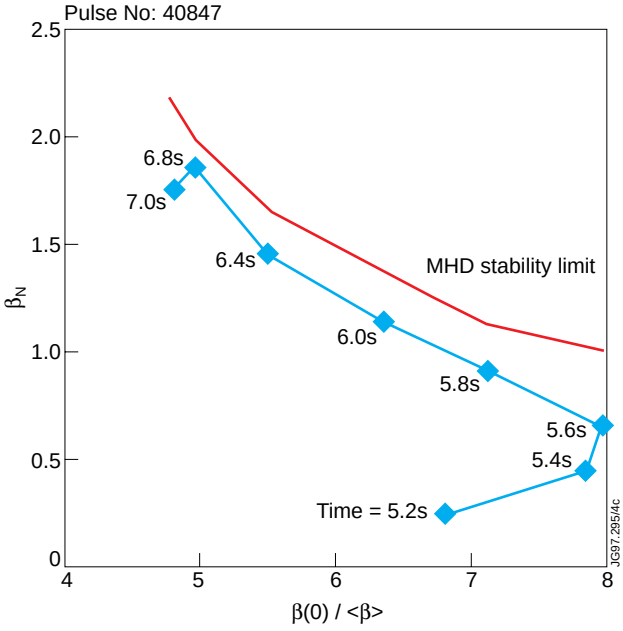

FIG. 23. Experimental and theoretical values of normalised β_N as a function of the pressure peaking factor during the evolution of an optimised shear discharge. The MHD stability boundary limit is also shown.

F. Alpha Particle Physics

ITER will, of course, be dependent for ignition and burn on the transfer back to the plasma of the energy from the alpha particles produced in DT fusion reactions. Thus, it is important to identify loss processes which could disturb the alpha heating; partly because of the effect on the plasma power balance but also because a significant loss of alphas from the plasma would lead to unacceptable loads on plasma facing surfaces.

The first consideration concerning alpha losses is to confirm the predictions of classical losses associated with the magnetic field configuration; or more specifically, due to the toroidal field ripple which arises from the finite number of coils. Classical losses can either be prompt, the ripple trapped particles going straight to the wall, or due to stochastic diffusion in the ripple fields. In order to test the effects of ripple losses, JET performed an experiment [28] in which the toroidal field ripple was increased by driving a current difference between alternate coils.

For the main part, the effects of TF ripple were as expected from classical calculations. In particular, it seems that alpha particles behave classically and that the heat loads on first wall

components are relatively straight forward to calculate using guiding centre codes. It is worthwhile noting that, whilst the effect of the ripple on error field locked modes was in accord with theory, losses of intermediate energy slowing-down NBI ions and the enhancement of the H-mode at ripple levels ~1% were unexpected. Neither is thought to be significant for ITER, though.

Over very many years, significant theoretical effort has concentrated on the effect of Toroidicity induced Alfven Eigenmodes (TAEs) on the alpha particle losses. Since alpha particles can be resonant with low (n,m) TAEs, a significant amount of drive for the instability is available and losses could be large. There are many driving and damping terms for these modes, making it imperative to study their growth and saturation mechanisms experimentally.

Work on this area in JET has proceeded on two fronts. The first is to drive these modes using the saddle coils [29], making it possible to measure damping rates when the modes are stable. Unfortunately, the saddle coils have suffered some technical problems and it has only been possible to collect a limited amount of data with them. An additional, peculiar difficulty has revolved around what was initially thought to be poor coupling between the saddle coils and n~1 TAEs in divertor plasmas. Subsequently, it has been realised that this effect is, in fact, due to stabilisation of this part of the spectrum by the plasma elongation and triangularity. Thus it has not been possible to make useful measurements of the effects on TAE growth or damping due to fast ions in divertor plasmas. In limiter plasmas, the increase in growth rate due to ICRH minority ions has been determined, using the saddle coils.

The other approach has been to make passive measurements of TAEs (and their ellipticity induced cousins, EAEs) using high frequency, magnetic pick-up coils. This has proven to be higly successful. TAEs with n~12 have been observed to be destabilised by slowing-down, NBI ions. TAEs with n~5 are predicted to be destabilised by ICRH minority ions and alpha-particles, both of which are in the MeV range. In the case of ICRH induced instability, a clear power threshold is observed, [30] as shown in figure 24. This is a clear indication that the fast ion β must exceed a threshold level in order to overcome the damping on thermal ions. This is even more starkly illustrated by alpha particle destabilisation of TAEs [31], in JET DT plasmas, as shown in figure 25. During the heating pulse, the alpha particles do not overcome the damping due to NBI and

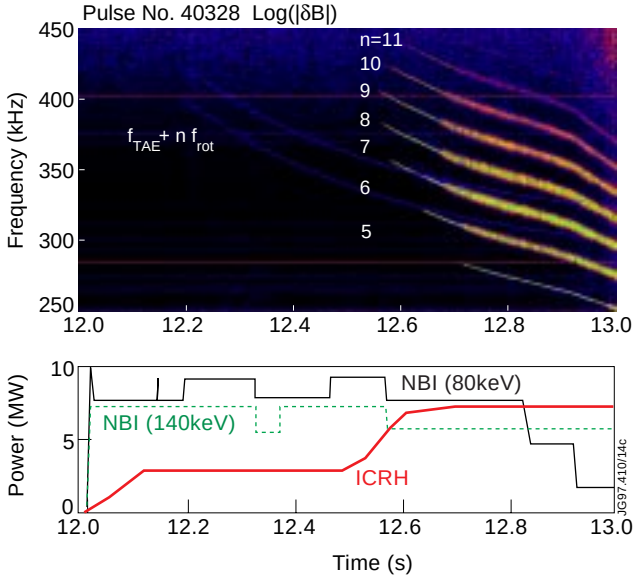

FIG. 24. Observation of power threshold of TAE modes excited by ICRH produced fast ions in deuterium plasmas with D-beams injection. ICRH power was increased in two steps as shown.

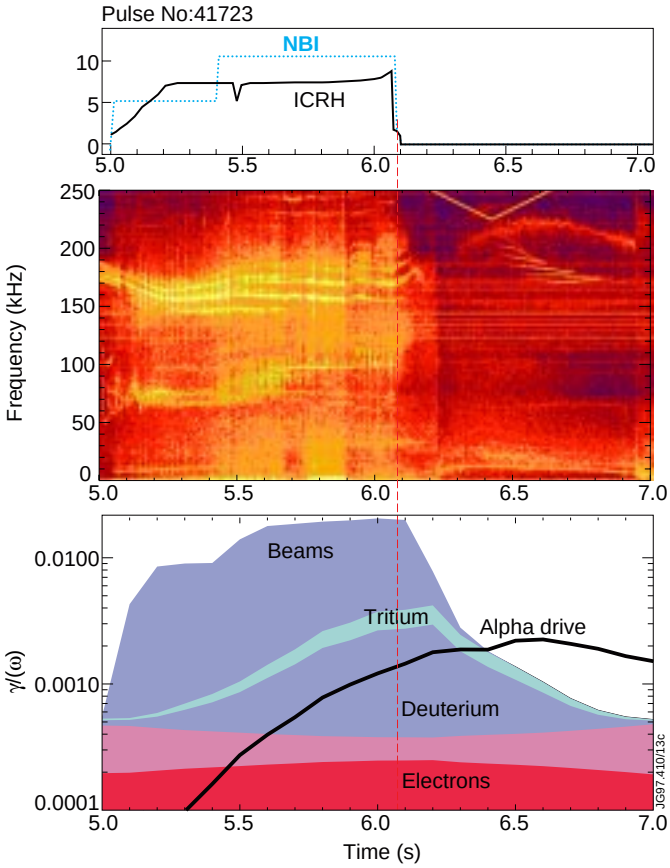

FIG. 25. A possible observation of α-particle driven TAE modes in the after glow of D-beam injected into 55:45 DT plasma. Six discrete modes can be seen in the expected frequency range of 200 kHz in the 6.5 and 7s time interval when the calculated damping rates becomes smaller than the α-drive.

thermal ions. However, when the heating is switched off, the longer slowing down time of the alphas means that they are able to destabilise the plasma, as seen in the figure. It is important to note that these observations are in very good accord with growth rates, computed using the CASTOR-K [32] and other codes. Thus important experimental benchmarking of TAE stability codes is being obtained in JET which will give confidence of their predictions for TAE behaviour in ITER.

It is believed that the highest performance DT shots will see TAE instability whilst the heating is still on. This will provide an important confirmation of the magnitude of the damping effects and will further enhance confidence in the code results. Beyond this, it is essential to study the saturation of TAEs because it is this which will determine their importance in ejecting particles from ITER.

III. DISCUSSION AND CONCLUSIONS

JET is presently in the DTE1 phase of its experimental programme. In the first phase of DTE1, significant results have been obtained where D-NBI, ICRF and LHCD additional heating power have been used. A significant part of the DT programme such as a study of wall change-over from D to T (DT mixture from 100:0 to 10:90), neutron calibration, ITER ρ*-scaling experiments (see Section 2.1 and 2.2 for H-mode threshold and confinement results), some trace tritium and ICRH experiments (see Section 2.3) have been carried out. Further, a neutral beam duct conditioning shot in which 11 MW T-beams were injected into a deuterium plasma produced 2.5 MW of peak fusion power and 6.9 MJ of fusion energy. The best optimised shear discharge with 10.5 MW of D-NBI and 8MW of ICRH produced 2 MW of fusion power and 2.9 MJ of fusion energy. However, the highest performance in terms of peak fusion power was achieved in a 3.3 MA discharge with ITER shape and q with 11MW of D-NB and 4 MW of ICRH. In all cases, there has been no attempt as yet to optimise the fusion yield by controlling

the D/T mixtures. Experiments in the second phase of DTE1 with full NBI (including D- and T-NBI) power and ICRH are imminent and are expected to significantly improve on the results of fusion power and Q obtained so far.

A budget of $2x10^{20}$ total number of neutrons has been set for the DTE1 experiments to limit the subsequent activation of the vessel. About 10% of this budget has been used up in the first phase of DTE1. The neutron budget limit constrains the number of DT shots consuming a large number of neutrons (long, high performance shots). The 20g of tritium available on-site permits a significant number of DT experiments in a series of JET sessions. The retrieved tritium is reprocessed by the on-site closed-circuit Active Gas Handling System for subsequent experiments anew.

In this paper, we have summarised the ITER relevant JET results obtained during the past year with MkIIa divertor including DT results obtained so far. The present JET programme to the end of 1999 continues to address the most critical physics issues that must be solved before the construction of ITER. These issues include L-H mode threshold power and energy confinement scaling in dimensionless parameters, long-pulse β-limits, α-particle effects, the effect of impurity seeding and a radiative divertor with low-heat flux and low target erosion. A series of divertor configurations with increasing closure are being studied to bring the ITER divertor concept to maturity. The next divertor, MkIIGB ('gas box'), will be installed by remote handling after the post DTE1 experiments. Thus, JET is also carrying out ITER-relevant technology activities such as the demonstration of remote handling and tritium technologies.

In conclusion, a combination of JET features such as large scale plasma (R_0 = 3m, plasma volume ~ 100 m3, plasma current 6MA), power full heating and current drive systems (NBI 22MW, ICRH 17MW , LHCD 10MW), ITER-like divertor configuration with low-Z materials (C and Be) for plasma facing components, skills in beryllium components design and handling, tritium compatibility and on-site reprocessing, remote handling and repair and finally operation in DT plasmas, make JET a unique device for making the most-relevant contributions to the ITER-design. This is clearly borne out from the results presented in the paper. The future experimental programme of JET is geared to obtain further results in the same direction.

ACKNOWLEDGEMENTS

We wish to thank the JET tokamak operation team, the NBI and ICRH plant teams, the AGHS group and those operating the diagnostics used in the experiments reported here.

REFERENCES

[1] The JET Design Team, The JET Project — Design Proposal, Rep. EUR-551e (EUR-JET-R5) (1976), Commission of the European Communities, Brussels.

[2] The JET Council, in the 4th Framework Research Programme of the European Communities, EUR FU 95 (1995), Commission of the European Communities, Brussels.
[3] ITER EDA Agreement and Protocol, IAEA, Vienna (1994); ITER Interim Design Report Package Documents, IAEA, Vienna (1996).
[4] BELL, A. et al., Paper presented at the 4th Int. Symp. on Fusion Nucl. Technology, Tokyo (1997) paper FT02, to be published in Fus. Tech.
[5] ROLFE, A., in Proc. of the 19th Symp. on Fus. Tech., Lisbon 1996, published by Elsevier (1997) 91.
[6] FALTER, H.D., Rep. JET-R(96)02, JET Joint Undertaking, Abingdon, UK (1996).
[7] REBUT, P.H. et al., Rep. JET-R(85)03, JET Joint Undertaking, Abingdon, UK (1985).
[8] ORLINSKIJ, D.V., MAGYAR, G., Nucl Fus. 28 (1988) 611.
[9] H-Mode Database Group, Proc. 21st EPS Conf. on Contr. Fus. Plasma Physics, Montpellier (1994), Europhysics conf. abstracts, vol. 18B, part I, 334.
[10] TAKIZIKA, T. and H-Mode Database Group, in Fusion Energy 1996 (Proc. 16th Int. Conf., 1996), IAEA, Vienna (1997), paper S-5, in press.
[11] RIGHI, E. et al, Paper presented at the IAEA H-Mode Physics Workshop, Kloster, Germany (1997), to be published.
[12] YUSHMANOV, P.N. et al., Nucl. Fus. 30 (1990) 1999.
[13] ITER H-Mode Database Working Group, Nucl. Fus. 34 (1994) 131.
[14] ITER Confinement Database and Modelling Working Group (presented by J.G. Cordey), Proc. 24th EPS Conf., Berchtesgaden (1997), to be published in Plasma Phys. Contr. Fus.
[15] CONNOR, J.W. and Taylor, J.B., Nucl. Fus. 17 (1977) 1047.
[16] JET Team (presented by J.G Cordey), in Fus. Energy 1996 (Proc. 16th Int. Conf., 1996), Vol. **1**, IAEA, Vienna (1997) 239.
[17] PETTY, C.C and LUCE, T.C., Proc. 24th EPS Conf., Berchtesgaden (1997), to be published. Also, CHRISTIANSEN, J.P. et al., ibid.
[18] JET Team (presented by J. Jacquinot), Proc. 5th IAEA Tech. Cttee. Mtg. on Alpha-Particles, JET, Abingdon, UK (1997).
[19] CALLEN, J.D. et al, Plasma Phys. and Contr. Nucl. Fus. Res, Kyoto (IAEA, Vienna, 1987) Vol. 2 157; HEGNA, C.C. et al., Plasma Phys. Contr. Fus. 35 (1993) 987.
[20] HUYSMANS, G.T.A., et al, Proc. 24th EPS Conf., Berchtesgaden, Germany (1997), to be published.
[21] JET Team (presented by M. Keilhacker), in Plasma Phys. and Contr. Nucl. Fus. Res. 1992 (Proc. 14th Int. Conf., 1992), Vol. **1**, IAEA, Vienna (1992) 15.
[22] JET Team (presented by M. Keilhacker), Proc. 24th EPS Conf., Berchtesgaden, Germany (1997), to be published in Plasma Phys. Contr. Fus.
[23] ZOHM, H. et al, Plasma Phys. Contr. Fus., 38 (1996) 105.
[24] MOHANTI, et al, Proc. 24th EPS Conf., Berchtesgaden, Germany (1997).

[25] BHATNAGAR, V.P. et al, *ibid.*
[26] LINGERTAT, J. , *ibid.*
[27] JET Team (presented by C. Gormezano), in Fus. Energy 1996 (Proc. 16th Int. Conf., 1996), Vol. **1**, IAEA, Vienna (1997) 487.
[28] TUBBING, B.J.D. et al, Proc. 22nd EPS Conf. on Contr. Fus. and Plasma Phys., Bournemouth (1995), Europhys. Conf. Abstracts, Vol. 19C, Part IV, 001.
[29] FASOLI, A. et al, Rep. JET-P(95)30, JET Joint Undertaking, Abingdon, UK (1995).
[30] FASOLI A. et al, Proc. 5th IAEA Tech. Cttee. Mtg. on Alpha-Particles, JET, Abingdon, UK (1997).
[31] BORBA, et al, Proc. 5th IAEA Tech. Cttee. Mtg. on Alpha-Particles, JET, Abingdon, UK (1997)
[32] KERNER, W. et al, Rep. JET-P(97)04, JET Joint Undertaking, Abingdon, UK (1997).